Functional importance of stripping in NFκB signaling revealed by a stripping-impaired IκBα mutant

Holly E. Dembinski[a], Kevin Wismer[a], Jesse D. Vargas[b,c], Gajendra W. Suryawanshi[b,c], Nadja Kern[a], Gerard Kroon[d], H. Jane Dyson[d], Alexander Hoffmann[b,c], and Elizabeth A. Komives[a,1]

[a]Department of Chemistry and Biochemistry, University of California, San Diego, La Jolla, CA 92093-0378; [b]Department of Microbiology, Immunology and Molecular Genetics, University of California, Los Angeles, CA 90095; [c]Institute for Quantitative Computational Biosciences, University of California, Los Angeles, CA 90095; and [d]Department of Integrative Structural and Computational Biology, The Scripps Research Institute, La Jolla, CA 92037

Edited by Gregory A. Petsko, Weill Cornell Medical College, New York, NY, and approved December 27, 2016 (received for review June 22, 2016)

Stress-response transcription factors such as NFκB turn on hundreds of genes and must have a mechanism for rapid cessation of transcriptional activation. We recently showed that the inhibitor of NFκB signaling, IκBα, dramatically accelerates the dissociation of NFκB from transcription sites, a process we have called "stripping." To test the role of the IκBα C-terminal PEST (rich in proline, glutamic acid, serine, and threonine residues) sequence in NFκB stripping, a mutant IκBα was generated in which five acidic PEST residues were mutated to their neutral analogs. This IκBα(5xPEST) mutant was impaired in stripping NFκB from DNA and formed a more stable intermediate ternary complex than that formed from IκBα(WT) because DNA dissociated more slowly. NMR and amide hydrogen–deuterium exchange mass spectrometry showed that the IκBα(5xPEST) appears to be "caught in the act of stripping" because it is not yet completely in the folded and NFκB-bound state. When the mutant was introduced into cells, the rate of postinduction IκBα-mediated export of NFκB from the nucleus decreased markedly.

transcription factor | binding kinetics | intrinsically disordered proteins | nuclear export | hydrogen–deuterium exchange

Stress-response transcription factors turn on hundreds of genes, and their regulation requires robust activation as well as rapid and complete cessation of the ensuing response. A good example is the NFκB family of transcription factors, which responds to a large number of extracellular stress stimuli, including factors controlling inflammation and the immune response (1–3). Aberrant regulation of NFκB results in numerous disease states, including cancer (1, 4). The IκB family of inhibitors keeps NFκB in the cytoplasm (in the "off" state) (5). IκBα is the main temporally regulated IκB. When a stress signal is received, IκBα is degraded rapidly, releasing NFκB, which enters the nucleus, binds to κB DNA sites, and up-regulates gene expression (Fig. 1*A*). In a classic negative feedback loop, the promoter upstream of the IκBα gene is strongly up-regulated by NFκB. We previously showed that in vitro IκBα rapidly accelerates the dissociation of NFκB from many different DNA sequences containing the κB motif in a folding-upon-binding event (6, 7). Thus, removal of NFκB(RelA/p50) from its target sites is kinetically determined, a process we call "molecular stripping" (8). The kinetic control of transcription factor–DNA interactions represents a paradigm shift because these interactions typically are described with equilibrium-binding models (9, 10) and thus would require the formulation of novel models based on stochastic rates.

For IκBα to strip NFκB from DNA, a ternary NFκB–DNA–IκBα complex must form at least transiently. A very transient NFκB–DNA–IκBα complex was indeed observed in stopped-flow fluorescence experiments (11). At high concentrations, signals corresponding to a ternary NFκB–DNA–IκBα complex were also observed by NMR (12, 13). Together the stopped-flow and NMR data showed that IκBα binds to the NFκB–DNA complex so tightly that it effectively does not dissociate, leading to a complex in which the DNA is bound to the N-terminal domains of NFκB and IκBα is bound to the dimerization domains.

IκBα, a protein with six ankyrin repeats (ARs), has a C-terminal sequence rich in proline (P), glutamic acid (E), serine (S), and threonine (T) residues (PEST) (Fig. 1*B*). The similarity of the IκBα PEST sequence to other negatively charged PEST sequences first suggested its involvement in degradation (14); however, more recent studies have not supported these claims and instead revealed degradation signals in the AR domain (15, 16). NMR studies showed that the PEST sequence interacts with positively charged residues in the DNA-binding pocket of NFκB (17), and simulations using a coarse-grained model showed that the IκBα PEST sequence electrostatically repels DNA from NFκB (8). The mutual exclusivity of DNA and PEST sequence binding to NFκB pointed to an involvement of the PEST in the stripping of NFκB from DNA; however, the obvious step of deleting the IκBα PEST sequence weakened NFκB binding (18), making the results of any stripping experiments equivocal. Instead, we neutralized the acidic IκBα PEST residues E282Q/E284Q/D285N/E286Q/E287Q to generate the IκBα(5xPEST) mutant, which bound NFκB with nearly WT affinity. This neutralized PEST version of IκBα is stripping impaired, allowing characterization of the NFκB–DNA–IκBα ternary complex. Here we present binding, structural, and single-cell imaging data showing that the IκBα(5xPEST) mutant accelerates the removal of NFκB from DNA at a much lower rate than the WT protein, that the ternary complex of the mutant persists even at low protein concentrations, and that the appearance of the newly formed NFκB–IκBα complex in the cytoplasm of intact cells is slowed for the IκBα(5xPEST) mutant compared with WT IκBα. These data collectively demonstrate the functional importance of IκBα-mediated stripping of NFκB from DNA in the kinetic control of NFκB signaling.

Significance

Stress-response transcription factors turn on hundreds of genes, and their activity must be turned off completely and quickly. The inhibitor protein IκBα turns off NFκB by forming a transient ternary complex with the NFκB–DNA complex and then promoting DNA dissociation (molecular stripping). Here we report a mutant IκBα that is impaired in its ability to strip NFκB from DNA. The mutant forms a more stable ternary complex, and biophysical characterization shows what IκBα looks like "in the act of stripping." We also show in single-cell nuclear export assays that the decrease in the rate of DNA dissociation from the mutant ternary complex matches the decrease in the rate of nuclear NFκB export in cells.

Author contributions: H.E.D., H.J.D., A.H., and E.A.K. designed research; H.E.D., K.W., J.D.V., G.W.S., N.K., and G.K. performed research; H.E.D., K.W., and J.D.V. analyzed data; and H.E.D. and E.A.K. wrote the paper.

The authors declare no conflict of interest.

This article is a PNAS Direct Submission.

[1]To whom correspondence should be addressed. Email: ekomives@ucsd.edu.

This article contains supporting information online at www.pnas.org/lookup/suppl/doi:10.1073/pnas.1610192114/-/DCSupplemental.

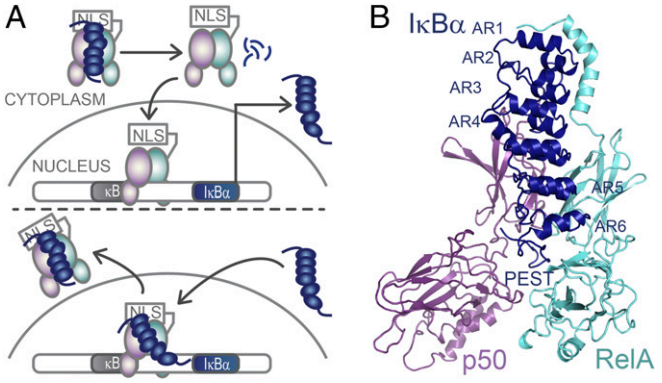

Fig. 1. IκBα regulates NFκB activity. (*A*) IκBα sequesters NFκB in the cytoplasm. When an extracellular stress signal (e.g., LPS, TNFα) is received, IκBα is phosphorylated by IKK, ubiquitinated, and degraded, thus revealing the NFκB nuclear localization signal (NLS), whereupon it enters the nucleus and binds to κB DNA sites. One of the genes under control of the κB promoter is IκBα, so newly synthesized IκBα then enters the nucleus, strips NFκB from DNA, and exports NFκB out of the nucleus. (*B*) Structural model of NFκB (RelA/p50) bound to the six-AR–containing IκBα showing the C-terminal PEST sequence [Protein Data Bank (PDB) 1IKN–1VKX composite] (25).

Results

Creation of Stripping-Impaired IκBα. Individual neutralization of each acidic IκBα PEST residue did not affect binding (Fig. S1 *A*–*C*) or the ability of each IκBα mutant to strip NFκB from DNA (Fig. S1*D*) (6). Subsequently, the five acidic IκBα PEST residues were neutralized collectively, generating IκBα(5xPEST). This mutant bound to NFκB dimerization domains with an affinity only fourfold lower than that of WT IκBα [NFκB–IκBα(WT) K_d = 0.38 (± 0.02) nM; NFκB–IκBα(5xPEST) K_d = 1.5 (± 0.3) nM) (Fig. S1*C*).

The mutant IκBα(5xPEST) appeared not to strip NFκB from DNA completely in stopped-flow fluorescence measurements (Fig. 2 *A* and *B*). The fluorescence signal decreased but plateaued at a higher value than for the WT protein. This behavior suggested that the IκBα(5xPEST) mutant was generating a more persistent ternary complex with NFκB and DNA. The leveling of the signal at a higher fluorescence suggested that the equilibrium between the NFκB–IκBα binary complex and the DNA-bound ternary complex had shifted toward the ternary complex compared with the result with WT IκBα. Steady-state fluorescence anisotropy was used to measure the binding affinity of a fluorescein-labeled IFN-κB hairpin DNA oligo (DNA^F) to NFκB, yielding a K_d of 32 ± 13 nM. The addition of IκBα(WT) diminished the DNA binding to a K_d of 170 ± 40 nM. DNA binding to the NFκB–IκBα(5xPEST) complex was intermediate, with a K_d of 64 ± 10 nM (Fig. 2 *C* and *D*).

Size-exclusion chromatography was used to evaluate whether the IκBα(5xPEST) mutant formed a stable ternary NFκB–DNA–IκBα(5xPEST) complex, but the DNA did not remain stably bound. EMSA showed that DNA bound more tightly to the NFκB–IκBα(5xPEST) complex than to the NFκB–IκBα(WT) complex, but neither complex bound DNA as tightly as NFκB alone (Fig. S2). Stopped-flow fluorescence showed that DNA dissociated from NFκB with a k_d (dissociation rate constant) of 0.6 ± 0.1/s, whereas DNA dissociated from the NFκB–DNA–IκBα(5xPEST) complex only slightly faster with a k_d of 1.7 ± 0.1/s. DNA dissociation from the NFκB–DNA–IκBα(WT) complex was too fast to measure directly, but using the measured K_d of 170 nM for DNA binding to the NFκB–IκBα(WT) complex and the previously measured DNA association rate for the NFκB–IκBα(WT) complex of $k_a = 8.6 \times 10^7$ M/s (11), we calculated the k_d for DNA dissociation from the ternary NFκB–DNA–IκBα(WT) complex to be 14.0 ± 0.1/s. Thus, WT IκBα efficiently mediates molecular stripping of NFκB from DNA by accelerating DNA dissociation from the ternary complex, whereas neutralization of the PEST sequence allows the DNA to remain bound (Fig. 2).

IκBα Accommodates DNA in the NFκB–DNA–IκBα(5xPEST) Ternary Complex with Structural Perturbations Radiating from AR5 and AR6 into AR3. Our group previously showed that AR5 and AR6 are disordered in free IκBα and fold upon binding to NFκB (19, 20). Cross-peaks for most of the amides in AR5 and AR6 were missing from the transverse relaxation-optimized heteronuclear single-quantum coherence (TROSY-HSQC) spectrum of free IκBα (19) but were observed for IκBα bound to NFκB (20). NMR studies in which excess DNA was added to the binary NFκB–IκBα(WT) complex also showed that the addition of DNA did not affect most of the resonances in AR1–AR4 but caused severe broadening of resonances in AR5 and AR6 (12).

We previously showed that DNA binding could be monitored by observing the 1D ^{1}H spectrum of the distinctive imino resonances of the DNA (13). We used this technique to monitor the formation of the ternary NFκB–DNA–IκBα(5xPEST) complex and found that the complex was fully formed at a slight excess (1.2-fold) of added DNA. Measurement of chemical-shift perturbation upon DNA binding by comparing the 800 MHz TROSY-HSQC spectrum of the binary NFκB–^{2}H^{15}N IκBα(5xPEST) complex with the spectrum of the ternary NFκB–DNA–^{2}H^{15}N IκBα(5xPEST) complex (Fig. 3*A*) revealed significant N–H chemical-shift perturbations throughout AR5 and AR6 in residues T219 (AR5), R245 (AR5), V246 (AR5), L256 (AR6), T257 (AR6), Q266 (AR6), and E284Q (PEST) (Fig. 3*B*). Significant chemical-shift perturbations extended up into AR3 to include residue Q165 (AR3). In addition to

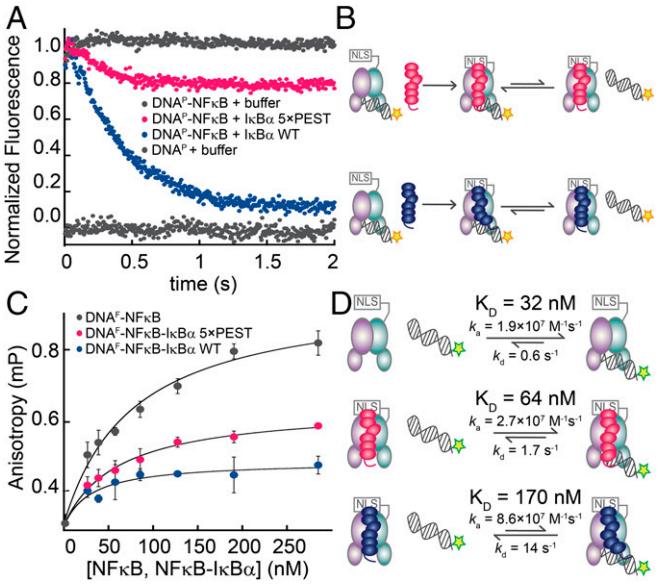

Fig. 2. The IκBα(5xPEST) mutant formed a stabilized NFκB–DNA–IκBα ternary complex. (*A*) Stopped-flow fluorescence traces corresponding to the dissociation of pyrene-labeled DNA (DNA^P) from NFκB. A fivefold excess of IκBα(WT) rapidly strips DNA^P from NFκB, whereas a fivefold excess of IκBα(5xPEST) retained bound DNA^P. For reference, traces of NFκB–DNA^P and DNA^P injected against buffer are shown at normalized fluorescence values of 1 and 0, respectively. (*B*) Schematic showing the reactions being monitored by the stopped-flow fluorescence experiment. The pyrene on DNA^P is indicated by a yellow star. (*C*) Equilibrium binding affinities were determined by monitoring the increase in steady-state fluorescence anisotropy of FITC-labeled DNA (DNA^F) as a function of the concentration of NFκB, NFκB–IκBα(5xPEST), or NFκB–IκBα(WT). (*D*) Schematic highlighting the rates and equilibrium binding affinities of DNA with NFκB, NFκB–IκBα(5xPEST), and NFκB–IκBα(WT). The stripping-impaired IκBα(5xPEST) complex shifts the equilibrium toward the ternary NFκB–DNA–IκBα complex. The fluorescein on DNA^F is indicated by a green star.

chemical-shift perturbations, amide resonances also disappeared upon the formation of the ternary complex; the great majority of the missing peaks were in AR3 (Table S1). Previous work had shown that some amide resonances (i.e., R143, G144, T146, Q154, C156, A158, S159, and T168) corresponding to AR3 are observed in free IκBα but not in the NFκB–IκBα binary complex (20). In addition to these missing peaks, N145, L150, A151, C152, L163, S174, and N180 were missing in the ternary NFκB–DNA–$^{2}H^{15}N$ IκBα(5xPEST) complex.

Although the addition of an excess of DNA caused the peaks corresponding to AR5 and AR6 to disappear in WT IκBα (12), most peaks were observed in the TROSY-HSQC spectrum of our ternary NFκB–DNA–$^{2}H^{15}N$ IκBα(5xPEST) complex. Only D226, Y251, S252, S258, G270, L272, and E275 were not observed; the rest of the peaks were observed, and most of the peaks corresponding to amide groups in the helical regions of AR5 and AR6 did not undergo significant chemical-shift perturbations.

Amide Exchange Revealed Changes in the Foldedness of IκBα(5xPEST) in the Ternary Complex. To explore the dynamic changes in IκBα upon the formation of the ternary complex further, we undertook amide hydrogen–deuterium exchange mass spectrometry (HDXMS) analysis. Consistent with the TROSY-HSQC chemical-shift perturbations, changes in amide exchange were observed in IκBα AR3, AR5, and AR6 (Fig. 4). IκBα residues 158–176 in AR3 showed increased exchange with IκBα(WT) and IκBα(5xPEST) upon formation of the ternary NFκB–DNA–IκBα complex; this region includes Q165, which also showed chemical-shift perturbation (Fig. 4*I*). IκBα residues 202–274 in AR5–AR6 showed increased exchange in the ternary NFκB–DNA–IκBα(5xPEST) complex compared with the binary complex; this region of IκBα also includes the AR5 and AR6 residues that showed significant chemical-shift perturbations (Fig. 4 *L–P*). IκBα residues 202–236 showed larger increases in amide exchange in the ternary complex formed with the IκBα(5xPEST) than in the ternary complex formed with IκBα(WT).

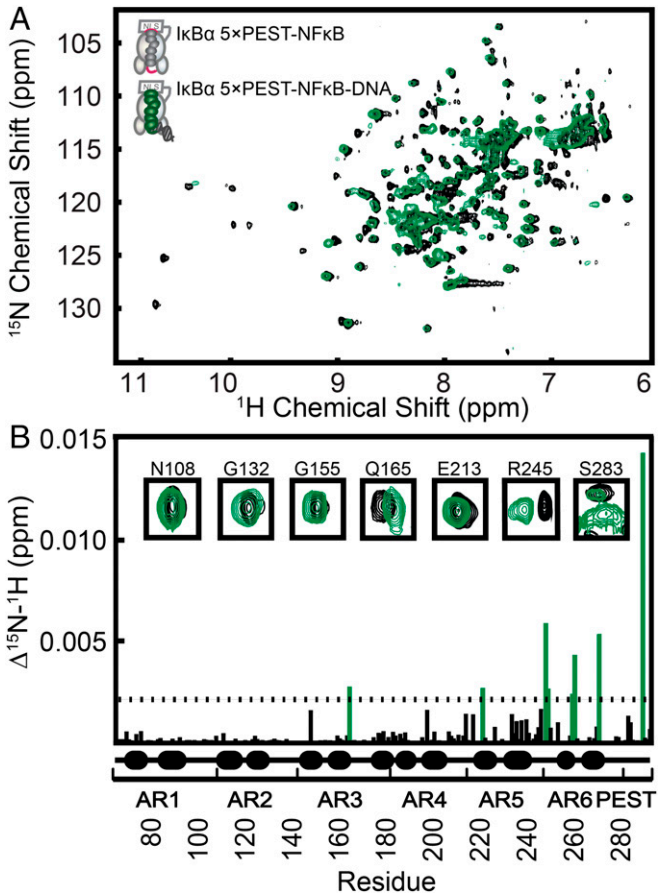

Fig. 3. TROSY-HSQC analysis revealed chemical-shift perturbations in IκBα AR3, AR5, and AR6 upon DNA binding to the NFκB–IκBα(5xPEST) complex. (*A*) Overlaid TROSY-HSQC spectra of the binary NFκB–$^{2}H^{15}N$ IκBα(5xPEST) complex and the ternary NFκB–DNA–$^{2}H^{15}N$ IκBα(5xPEST) complex. (*B*) Chemical-shift perturbations as a function of residue number. Residues for which DNA binding resulted in a chemical-shift perturbation of more than one SD from the mean were Q165 (AR3), T219 (AR5), R245 (AR5), V246 (AR5), L256 (AR6), T257 (AR6), Q266 (AR6), and E284Q (PEST). Resonances that disappeared upon DNA binding were E128 (AR2), R140 (AR3), N182 (AR4), D226 (AR5), Y251 (AR6), S252 (AR6), W258 (AR6), G270 (AR6), L272 (AR6), and E275 (AR6). The insets show a selection of peaks corresponding to each AR.

Collectively, the chemical-shift perturbation data and amide HDXMS form a consistent structural picture of the stabilized ternary NFκB–DNA–IκBα complex that accommodates the presence of DNA by subtle structural adjustments in AR3, AR5, and AR6 (Fig. 5).

To ascertain whether there were differences in the IκBα(5xPEST) and IκBα(WT) interactions with NFκB, we analyzed the NFκB peptides from the binary NFκB–IκBα and ternary NFκB–DNA–IκBα complexes of both IκBα(WT) and IκBα(5xPEST) (Fig. S3). No discernable differences in amide exchange were observed in the NFκB peptides, providing a strong confirmation that the IκBα(5xPEST) mutant forms a ternary complex that is highly similar to the IκBα(WT) ternary complex.

Previous NMR studies revealed inaccuracies in the IκBα PEST sequence–NFκB contacts displayed in crystal structures (21, 22) and suggested that the PEST sequence instead contacts R33 and R35 in the RelA DNA-binding domain (17). The HDXMS data showed that the IκBα(WT)PEST sequence was less dynamic than the PEST sequence of the IκBα(5xPEST) mutant (Fig. 4*R*). These data support the notion that electrostatic contacts between the IκBα PEST sequence and the positively charged DNA-binding loops batten down the C terminus of IκBα(WT) in NFκB binding and that these interactions are abolished in the IκBα(5xPEST) mutant.

Stripping-Impaired IκBα Is Deficient in Regulating NFκB in Knock-Out Mouse Embryonic Fibroblast Cells. To ascertain the functional ramifications of the increased ternary complex stabilization, we generated $IκBα^{-/-}β^{-/-}ε^{-/-}RelA^{-/-}$ mouse embryonic fibroblasts (MEFs) that lack all three classical NFκB inhibitors and RelA and reconstituted them with a constitutively expressed fluorescent GFP-RelA and NFκB-responsively expressed IκBα(WT) or IκBα(5xPEST) as described previously (23). EMSA analysis showed the IκBα(5xPEST) normally was localized in resting cells and after TNF stimulation (Fig. S4). As previously shown (23), when WT IκBα was expressed after a pulse of TNFα, single-cell traces showed that GFP–NFκB entered the nucleus and was exported rapidly back into the cytoplasm (Fig. 6). In stark contrast, when IκBα(5xPEST) was expressed following the TNFα pulse, single-cell traces showed that GFP–NFκB remained in the nucleus. In fact, the results from the IκBα(5xPEST) mutant resembled previous results with IκBβ (23), which is known to persist in the nucleus (24). The average rate of GFP–NFκB nuclear export for IκBα(WT) was 2.0 ($\pm$ 0.2) $\times$ 10^{-2}/min, whereas the IκBα(5xPEST) transfectants had a ninefold slower rate of GFP–NFκB nuclear export of 2.2 ($\pm$ 0.1) $\times$ 10^{-3}/min.

Discussion

IκBα(WT) efficiently strips NFκB from DNA (6, 11). The mechanism of this process necessitates the formation of a ternary complex, which was extremely transient under stopped-flow conditions but could be observed under the high-concentration conditions of NMR experiments (11–13). Using coarse-grained simulations, we showed that at least part of the driving force for molecular stripping likely comes from electrostatic repulsion between the negatively charged IκBα PEST sequence and DNA (25).

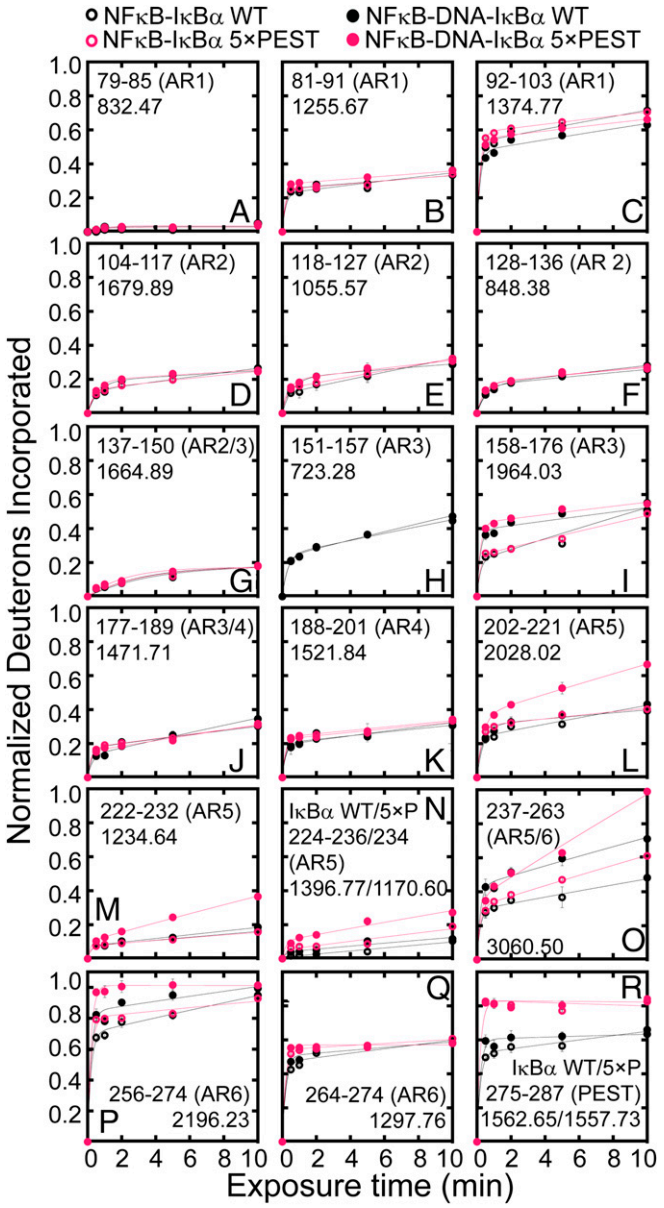

Fig. 4. The NFκB–IκBα(5xPEST) complex exhibited increased amide H/D exchange in IκBα AR3, AR5, and AR6 upon DNA binding. (*A–H*, *J*, *K*, and *Q*) DNA binding did not affect amide exchange in AR1, AR2, and AR4. (*I*, *O*, and *P*) DNA binding increased amide exchange in IκBα residues 158–176 of AR3 and residues 237–274 of AR5 and AR6 in both NFκB–DNA–IκBα(WT) and NFκB–DNA–IκBα(5xPEST). (*L–N*) DNA binding caused increased exchange in IκBα AR5 and AR6 in the NFκB–DNA–IκBα(5xPEST) complex compared with the ternary NFκB–DNA–IκBα(WT), binary NFκB–IκBα(5xPEST), and binary NFκB–IκBα(WT) complexes. (*R*) The PEST sequence of IκBα(5xPEST) exchanged more than the PEST sequence of IκBα(WT); however, the addition of DNA did not significantly alter exchange in the PEST regions.

Here, we undertook a comprehensive experimental characterization of the effects of PEST neutralization on the kinetics of molecular stripping, on the structure of the transient ternary complex, and on the function of IκBα. By neutralizing the PEST sequence, we were able to ascribe a clear function to the IκBα PEST sequence, definitively resolving previously confusing reports. Our results reveal that the negatively charged PEST residues actually function to promote stripping of NFκB from DNA.

Using stopped-flow fluorescence and equilibrium steady-state anisotropy, we showed that DNA dissociates less readily from the NFκB–DNA–IκBα(5xPEST) ternary complex. On the other hand, a stable ternary complex was not observed. Instead, an equilibrium mixture of the binary NFκB–IκBα and ternary NFκB–IκBα–DNA complexes forms, and the 5xPEST mutations shift the equilibrium toward the ternary complex (Fig. 2*D*). DNA dissociates eightfold more slowly from the PEST-neutralized ternary complex and also associates more slowly with the WT ternary complex; both are consistent with electrostatic repulsion between the IκBα PEST sequence and the DNA.

As a result of this shifted equilibrium toward the ternary NFκB–DNA–IκBα(5xPEST) complex, we were able to characterize the ternary complex, which is the necessary intermediate in the IκBα-mediated stripping of NFκB from the DNA. Importantly, HDXMS analysis of NFκB in both the IκBα(WT) and IκBα(5xPEST) binary and ternary complexes showed no differences in amide exchange of the NFκB in complex with either IκBα(WT) or IκBα(5xPEST) (Fig. S3). Both kinetic experiments and NMR characterization of the ternary complex in the presence of excess DNA showed that IκBα does not dissociate from NFκB once it is bound (11–13, 26). Here we show that in the stabilized ternary complex formed with the IκBα(5xPEST) mutant, chemical shifts for most IκBα residues in AR1–AR4 were unperturbed in the binary NFκB–IκBα and ternary NFκB–DNA–IκBα complexes. Resonances in AR5 and AR6, particularly in the β-hairpins and loops, had significantly different chemical shifts in the ternary and binary complexes, but the helices remained largely unperturbed (Fig. 5).

The AR domain of IκBα appears to make both structural and dynamic changes to accommodate DNA in the ternary complex. Amide HDXMS experiments revealed that wherever NMR chemical shifts were perturbed, indicating local structural changes, amide exchange increased, corresponding to increased dynamics in the ternary complex (Fig. 5). These results strongly suggest that the structure of the ternary complex is, in fact, an intermediate in the coupled folding and binding of IκBα to NFκB and that IκBα begins to fold during stripping, but folding is not completed until DNA dissociates.

Throughout AR5 and AR6, amide exchange is increased in the ternary complex, indicating that these two repeats, which fold on binding to NFκB (27), are partially unfolded in the ternary complex. These results also help explain the origins of the line broadening previously observed in NMR experiments on the ternary complex (12). The structural accommodation of the DNA by IκBα radiates via long-range allostery into AR3, which is the most stably folded region of free IκBα (28). Previous NMR experiments showed that resonances in AR3 broaden upon NFκB binding (20),

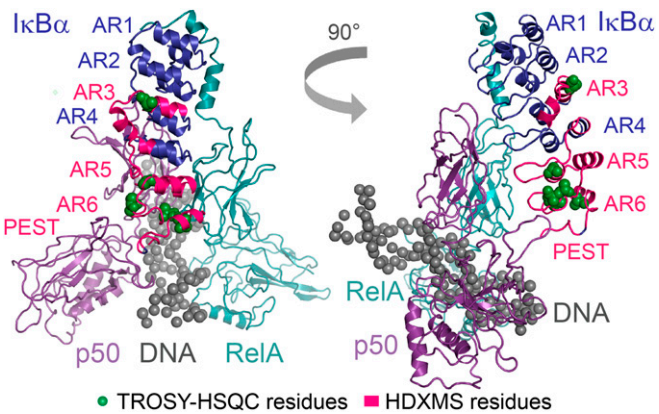

Fig. 5. Upon the addition of DNA to form the NFκB–DNA–IκBα(5xPEST) ternary complex, significant chemical-shift perturbations and increased amide exchange localize to the same regions of AR3, AR5, and AR6. Results are displayed on the PDB 1IKN–1VKX composite of RelA, p50, IgκB DNA, and IκBα (25).

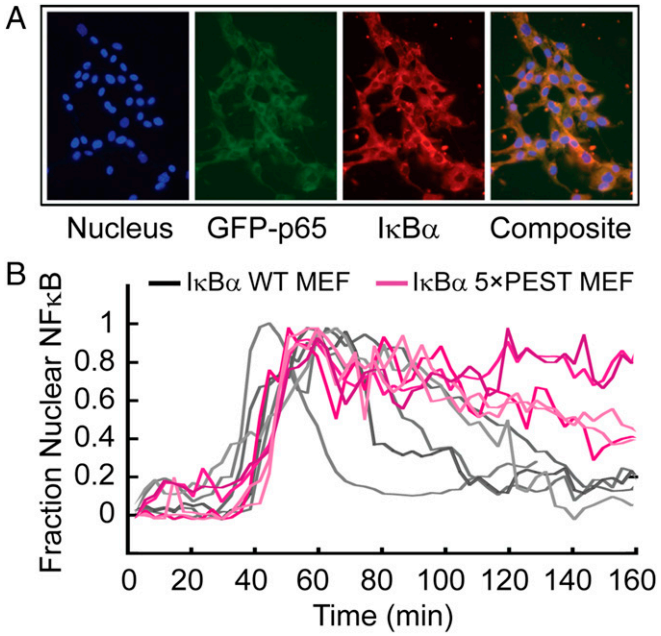

Fig. 6. The IκBα(5xPEST) mutant caused GFP–NFκB to be retained in the nucleus of live $I\kappa B\alpha^{-/-}\beta^{-/-}\varepsilon^{-/-}$ $RelA^{-/-}$ MEFs. (*A*) MEFs expressing IκBα(5xPEST) behind the native κB promoter were visualized for Hoechst-stained nuclei, GFP–RelA, and mCherry-fused IκBα antibody showing colocalization of RelA and IκBα (Composite). (*B*) After a pulse of TNFα, the same cells showed a markedly diminished rate of export of GFP–NFκB from the nucleus when IκBα(5xPEST) replaced IκBα(WT).

and our results suggest DNA binding further weakens the AR3 structure. Previous single-molecule FRET studies suggested that AR3 senses events at the N-terminal domains of NFκB; in these studies, a subtle twisting of the AR domain accounted for the observed decrease in the FRET signal when the N-terminal domains were included in the binary complex and pointed to a slight structural rearrangement upon formation of the binary NFκB–IκBα complex (29). Here we see that when the ternary complex forms, AR3 senses what is bound to the NFκB N-terminal domains—in this case, DNA.

The ternary complex formed with IκBα(5xPEST) is indeed more stable than that formed with IκBα(WT), particularly from the standpoint of the DNA. We knew that IκBα does not dissociate from NFκB once bound, but here we show that DNA association with and dissociation from the ternary complex is very sensitive to electrostatic repulsion by the PEST sequence. When newly synthesized WT IκBα enters the nucleus and binds to DNA-bound NFκB, it causes DNA to dissociate at a rate of ~14/s, which is sufficient to trigger rapid export of all the NFκB from the nucleus. By contrast, the stripping-impaired mutant shows an eightfold slower dissociation rate of DNA from the ternary complex. Intracellular nuclear export assays showed a similar decrease in the rate of export of NFκB from the nucleus when IκBα(5xPEST) replaced IκBα(WT) in intact cells. We conclude that molecular stripping of NFκB from DNA is most likely the only kinetic step responsible for the rapid rate of NFκB removal from the nucleus. Simply neutralizing five negatively charged residues within the PEST sequence of IκBα alters the DNA K_d to prolong the nuclear residence time by an order of magnitude. These results reveal how finely tuned the kinetic processes are in the NFκB signaling system. More importantly, they provide strong evidence for the functional significance of molecular stripping in controlling this important, stress-induced transcriptional response.

Materials and Methods

Protein Expression and Purification. Human $I\kappa B\alpha_{67-287}$ (IκBα) mutants were produced using site-directed mutagenesis, and the proteins were expressed and purified as described (30). $^{2}H^{15}N$-labeled IκBα(WT) and $^{2}H^{15}N$-labeled IκBα(5xPEST) were expressed in *Escherichia coli* BL21 DE3 cells (Agilent) grown in M9 minimal medium in D_2O (Cambridge Isotope Laboratories) supplemented with 2 g/L $^{15}NH_4Cl$ (Cambridge Isotope Laboratories) as described (31). Murine N-terminal hexahistidine-$RelA_{19-321}$/$p50_{39-350}$ heterodimer (NFκB) was coexpressed as described previously (20) and was purified by nickel affinity chromatography, cation exchange chromatography (Mono S; GE Healthcare), and size-exclusion chromatography (Superdex 200; GE Healthcare). Murine dimerization domain $RelA_{190-321}$ with an N-terminal cysteine and dimerization domain $p50_{248-350}$ were expressed, purified, and prepared for surface plasmon resonance (SPR) as described (25, 26, 29, 30). Immediately before the experiments, IκBα was purified by size-exclusion chromatography (Superdex 75; GE Healthcare), and NFκB and NFκB-IκBα complexes were purified by size-exclusion chromatography (Superdex 200) in 25 mM Tris (pH 7.5), 150 mM NaCl, 1 mM DTT, and 0.5 mM EDTA. Protein concentrations were determined by spectrophotometry at 280 nm (NFκB: ε = 43,760 M/cm; IκBα: ε = 12,950 M/cm).

DNA Labeling and Purification. A hairpin DNA sequence corresponding to the IFN-κB site with a 5′ amino modification, 5′-AmMC6/GGGAAATTCCTCCCC-CAGGAATTTCCC-3′ (IDT Technologies), was labeled with pyrene (*N*-hydroxyl succinimide ester) (DNA^P) (Sigma) or fluorescein (fluorescein isothiocyanate, Sigma) (DNA^F) as described (32).

Stopped-Flow Fluorescence. Stopped-flow fluorescence experiments were performed on an Applied Photophysics SX-20 stop-flow apparatus at 25 °C collecting 2,000 points linearly to a final mixing volume of 200 μL. The IκBα-mediated dissociation of DNA^P from NFκB was observed by adding increasing concentrations of IκBα (0.25, 0.50, 0.75, 1.00, 1.25, 1.50, 1.75, and 2.00 μM) to an NFκB (0.10 μM)–DNA^P (0.12 μM) complex and monitoring the change in fluorescence of the DNA^P. The pyrene label was excited at 343 nm, with emission monitored at 376 nm with a 350-nm–cutoff filter. The dissociation of DNA from the ternary complex was observed by adding a 50-fold excess (6 μM) unlabeled IFN-κB DNA oligo to the preformed NFκB (0.1 μM)–DNA^P (0.12 μM)–IκBα (0.12 μM) complex. The association of IκBα with NFκB or NFκB-DNA was observed via the native Trp fluorescence of Trp-258 in IκBα, exciting at 280 nm and monitoring emission at 345–355 nm with a 320-nm–cutoff filter. Increasing concentrations of NFκB or NFκB–DNA (0.30, 0.40, 0.50, 0.60, 0.70, and 0.80 μM) were mixed with IκBα (0.10 μM). Data were analyzed with pro Fit 6.1.14 (Quansoft, Inc.) (30).

Fluorescence Anisotropy. DNA^F (5 nM) was incubated with increasing concentrations of NFκB, NFκB–IκBα(WT), or NFκB–IκBα(5xPEST) (0.0, 25.3, 38.0, 57.0, 85.4, 128.1, 192.2, and 288.3 nM) for 4 h at 4 °C before data collection in triplicate at 25 °C on a Beckman Coulter DTX 880 Multimode Detector by exciting DNA^F at 495 nm and monitoring emission at 519 nm. Anisotropy values were calculated according to the equation $r = [I_{(V,V)} - GI_{(V,H)}]/[I_{(V,V)} - 2GI_{(V,H)}]$, where r is anisotropy, $I_{(V,V)}$ is the fluorescence intensity in the parallel direction, $I_{(V,H)}$ is the fluorescence intensity in the perpendicular direction, and G of 0.67 (33). The binding curves were fit to the equation: $A = (A_{max}\,[P])/(K_d + [P]) + b$, where A is the fluorescence anisotropy value, A_{max} is the maximum anisotropy, [P] is protein concentration, K_d is the equilibrium dissociation constant, and b is the y-intercept.

SPR Experiments. Sensorgrams were recorded on a GE Biacore 3000 instrument using streptavidin chips (GE Healthcare) by immobilizing 150, 250, and 350 response units of $p50_{dd}$/biotin-$RelA_{dd}$ on flow cells 2, 3, and 4, respectively, leaving flow cell 1 unmodified for reference subtraction. NFκB-binding experiments were conducted on IκBα(WT) and IκBα(5xPEST), and the data were analyzed as described (18, 30).

EMSA. Binding reactions contained 30 μM FITC–DNA or 6 μM RelA/p50 and 30 μM FITC–DNA (incubated for 20 min in the dark at 25 °C) to which a 1.2-fold excess of IκBα(WT), a 1.2-fold excess of IκBα(5×PEST), or buffer was added to bring the final reaction volume to 20 μL. The reaction mixtures (10 μL) were added to 10 μL 2× loading buffer [40 mM Tris (pH 8.0), 100 mM NaCl, 2 mM $MgCl_2$, 2 mM DTT, 0.5 mg/mL BSA, 10% glycerol, 0.001% (wt/vol) bromophenol blue] and were incubated for 1 h in the dark at 25 °C. The reaction mixtures were run on a 6% polyacrylamide nondenaturing gel containing 25 mM Tris·HCl (pH 8.3), 2.5% glycerol, 19 mM glycine, and 1 mM DTT at 40 V for 4 h at 25 °C in the dark. The gel was visualized via UV transillumination and quantified using Image J.

NMR. The binary complexes of NFκB with $^{2}H^{15}N$ IκBα(WT) or $^{2}H^{15}N$ IκBα(5xPEST) were purified by size-exclusion chromatography (Superdex 200). For the ternary NFκB–DNA–$^{2}H^{15}N$ IκBα(5xPEST) complex, NFκB was incubated in a 1.2-fold excess of DNA, and an equimolar concentration of $^{2}H^{15}N$ IκBα(5xPEST) was added to the NFκB–DNA complex. Samples were exchanged into 25 mM D-Tris (pH 7.5), 50 mM NaCl, 1 mM EDTA, 1 mM DTT, 90% H_2O, 10% D_2O via PD-10 desalting columns (GE Healthcare) and were concentrated to 0.12 mM using polyethersulfone Vivaspin 6 concentrators (Sartorius). TROSY-HSQC spectra were collected at 30 °C on a Bruker Avance 800-MHz spectrometer equipped with a cryoprobe with 256 scans and 2,048 (t2) × 128 (t1) complex points.

The NFκB–$^{2}H^{15}N$–IκBα(WT) complex had been assigned previously (20), and these assignments were used to assign the nearly identical TROSY-HSQC spectra of the NFκB–$^{2}H^{15}N$ IκBα(5xPEST) complex (78.6% assigned) and the NFκB–DNA–$^{2}H^{15}N$ IκBα(5xPEST) complex (74.3% assigned). The four IκBα(5xPEST) mutant residues, E282Q, E284Q, D285N, and E286Q, in the NFκB–$^{2}H^{15}N$ IκBα(5xPEST) and NFκB–DNA–$^{2}H^{15}N$ IκBα(5xPEST) spectra were also assigned by comparison with the WT spectra. Chemical-shift perturbations were calculated by the equation $[(\Delta\delta HN)^2 + (\Delta\delta NH)^2/25]/2)^{1/2}$, and those exceeding one SD from the mean were deemed significant.

HDXMS. HDXMS was performed using a Waters G2Si mass spectrometer with HD/X technology. The NFκB–DNA–IκBα(WT) and NFκB–DNA–IκBα(5xPEST) samples were prepared by overnight incubation of NFκB in a 10-fold excess of the unmodified IFN-κB hairpin DNA followed by the addition of IκBα(WT) or IκBα(5xPEST). The final concentrations were as follows: NFκB (5 μM):DNA (50 μM):IκBα(WT) (5 μM) or NFκB (5 μM):DNA (50 μM):IκBα(5xPEST) (5 μM). For each deuteration time, 4 μL of the complex was equilibrated to 25 °C for 5 min and then was mixed with 56 μL D_2O buffer [25 mM Tris (pH 7.5), 150 mM NaCl, 1 mM DTT, 0.5 mM EDTA in D_2O] for 0, 0.5, 1, 2, 5, or 10 min. The exchange was quenched with an equal volume of quench solution (3 M guanidine, 0.1% formic acid, pH 2.66). The quenched sample (50 μL) was injected into an in-line pepsin column (immobilized pepsin; Pierce, Inc.) at 15 °C. The resulting peptides were captured on a BEH C18 VanGuard Precolumn and then were separated on an Acquity UPLC BEH C18 column (1.7 μM, 1.0 × 50 mm; Waters Corporation) using a 7–85% acetonitrile gradient in 0.1% formic acid over 7.5 min and were electrosprayed into the mass spectrometer. Data were collected in the Mobility, ESI+ mode with a mass acquisition range of 200–2,000 (*m/z*) and a scan time 0.4 s with continuous lock-mass correction. For peptide identification, the mass spectrometer was set to collect data in the MS^E, ESI+ mode instead.

The peptides were identified from triplicate MS^E analyses of 10 μM IκBα(WT), IκBα(5xPEST), or NFκB, and data were analyzed using PLGS 2.5 (Waters Corporation) as previously described (29). The peptides identified in PLGS then were analyzed in DynamX 3.0 (Waters Corporation) following previously published methods (29, 34).

Intracellular NFκB Nuclear Export Experiments. Nuclear translocation experiments were performed as described previously (23). Briefly, NFκB-inducible IκBα constructs were derived from an MFG-derived self-inactivating retrovirus backbone (HRSpuro) modified to express the IκBα transgene under the control of five tandem κB sites upstream of a minimal promoter. AcGFP1 was fused to the N terminus of RelA, and the resulting construct was subcloned into the constitutively expressing retroviral plasmid pBabe-Hygro.

Plat-E cells (Cell Biolabs, Inc.) were transfected together with Lipofectamine 2000 transfection reagent (Invitrogen) for 48 h. The supernatant was filtered and used to infect *IκBα*$^{-/-}$*β*$^{-/-}$*ε*$^{-/-}$ *RelA*$^{-/-}$ MEFs. Transduced cells were selected with hygromycin hydrochloride (Sigma) for AcGFP–RelA and with puromycin hydrochloride (Sigma) for IκBα constructs. Cells were plated onto 35-mm glass-bottomed dishes (MatTek) or ibidi eight-well chambers (ibidi GmbH) 24 h before stimulation and immediate imaging.

Images were acquired on an Axio Observer Z1 inverted microscope (Carl Zeiss Microscopy GmbH) with a 40×, 1.3 NA oil-immersion or a 20×, 0.8 NA air-immersion objective equipped with a CoolSNAP HQ2 CCD camera (Photometrics) using ZEN imaging software (Carl Zeiss Microscopy GmbH). Environmental conditions were maintained in a humidified chamber at 37 °C, 5% CO_2 (PeCon). Quantitative image processing was performed using the FIJI distribution of Image J (NIH). All cells in each frame in the microscope imaging experiments were measured for total fluorescence intensity. Time-course data were normalized by the minimum and maximum values to account for the varying overall intensities of different cells. The single-cell traces were averaged, and the data from 60–160 min were fit to a single exponential decay. The fitted rate and corresponding error of the fit are reported.

ACKNOWLEDGMENTS. This work was supported by NIH Grant P01-GM071862 (to E.A.K., H.J.D., and A.H.).

1. Ghosh S, May MJ, Kopp EB (1998) NF-kappa B and Rel proteins: Evolutionarily conserved mediators of immune responses. *Annu Rev Immunol* 16:225–260.
2. Hoffmann A, Baltimore D (2006) Circuitry of nuclear factor kappaB signaling. *Immunol Rev* 210:171–186.
3. Hoffmann A, Levchenko A, Scott ML, Baltimore D (2002) The IkappaB-NF-kappaB signaling module: Temporal control and selective gene activation. *Science* 298(5596):1241–1245.
4. Kumar A, Takada Y, Boriek AM, Aggarwal BB (2004) Nuclear factor-kappaB: Its role in health and disease. *J Mol Med (Berl)* 82(7):434–448.
5. Baeuerle PA, Baltimore D (1988) I kappa B: A specific inhibitor of the NF-kappa B transcription factor. *Science* 242(4878):540–546.
6. Bergqvist S, et al. (2009) Kinetic enhancement of NF-kappaBxDNA dissociation by IkappaBalpha. *Proc Natl Acad Sci USA* 106(46):19328–19333.
7. Ferreiro DU, Komives E (2010) Molecular mechanisms of system control of NF-κB signaling by IκBα. *Biochemistry* 49(8):1560–1567.
8. Potoyan DA, Zheng W, Ferreiro DU, Wolynes PG, Komives EA (2016) PEST control of molecular stripping of NFκB from DNA transcription sites. *J Phys Chem B* 120(33):8532–8538.
9. Bintu L, et al. (2005) Transcriptional regulation by the numbers: Models. *Curr Opin Genet Dev* 15(2):116–124.
10. Siggers T, et al. (2011) Principles of dimer-specific gene regulation revealed by a comprehensive characterization of NF-κB family DNA binding. *Nat Immunol* 13(1):95–102.
11. Alverdi V, Hetrick B, Joseph S, Komives EA (2014) Direct observation of a transient ternary complex during IκBα-mediated dissociation of NF-κB from DNA. *Proc Natl Acad Sci USA* 111(1):225–230.
12. Sue SC, Alverdi V, Komives EA, Dyson HJ (2011) Detection of a ternary complex of NF-kappaB and IkappaBalpha with DNA provides insights into how IkappaBalpha removes NF-kappaB from transcription sites. *Proc Natl Acad Sci USA* 108(4):1367–1372.
13. Mukherjee SP, Quintas PO, McNulty R, Komives EA, Dyson HJ (2016) Structural characterization of the ternary complex that mediates termination of NF-κB signaling by IκBα. *Proc Natl Acad Sci USA* 113(22):6212–6217.
14. Kato T, Jr, Delhase M, Hoffmann A, Karin M (2003) CK2 is a C-terminal IkappaB kinase responsible for NF-kappaB activation during the UV response. *Mol Cell* 12(4):829–839.
15. Mathes E, Wang L, Komives E, Ghosh G (2010) Flexible regions within IkappaBalpha create the ubiquitin-independent degradation signal. *J Biol Chem* 285(43):32927–32936.
16. Fortmann KT, Lewis RD, Ngo KA, Fagerlund R, Hoffmann A (2015) A regulated, ubiquitin-independent degron in IκBα. *J Mol Biol* 427(17):2748–2756.
17. Sue SC, Dyson HJ (2009) Interaction of the IkappaBalpha C-terminal PEST sequence with NF-kappaB: Insights into the inhibition of NF-kappaB DNA binding by IkappaBalpha. *J Mol Biol* 388(4):824–838.
18. Bergqvist S, Ghosh G, Komives EA (2008) The IkappaBalpha/NF-kappaB complex has two hot spots, one at either end of the interface. *Protein Sci* 17(12):2051–2058.
19. Cervantes CF, Handley LD, Sue SC, Dyson HJ, Komives EA (2013) Long-range effects and functional consequences of stabilizing mutations in the ankyrin repeat domain of IκBα. *J Mol Biol* 425(5):902–913.
20. Sue SC, Cervantes C, Komives EA, Dyson HJ (2008) Transfer of flexibility between ankyrin repeats in IkappaB* upon formation of the NF-kappaB complex. *J Mol Biol* 380(5):917–931.
21. Huxford T, Huang DB, Malek S, Ghosh G (1998) The crystal structure of the IkappaBalpha/NF-kappaB complex reveals mechanisms of NF-kappaB inactivation. *Cell* 95(6):759–770.
22. Jacobs MD, Harrison SC (1998) Structure of an IkappaBalpha/NF-kappaB complex. *Cell* 95(6):749–758.
23. Fagerlund R, et al. (2015) Anatomy of a negative feedback loop: The case of IκBα. *J R Soc Interface* 12(110):0262.
24. Rao P, et al. (2010) IkappaBbeta acts to inhibit and activate gene expression during the inflammatory response. *Nature* 466(7310):1115–1119.
25. Potoyan DA, Zheng W, Komives EA, Wolynes PG (2016) Molecular stripping in the NF-κB/IκB/DNA genetic regulatory network. *Proc Natl Acad Sci USA* 113(1):110–115.
26. Bergqvist S, et al. (2006) Thermodynamics reveal that helix four in the NLS of NF-kappaB p65 anchors IkappaBalpha, forming a very stable complex. *J Mol Biol* 360(2):421–434.
27. Truhlar SM, Torpey JW, Komives EA (2006) Regions of IkappaBalpha that are critical for its inhibition of NF-kappaB.DNA interaction fold upon binding to NF-kappaB. *Proc Natl Acad Sci USA* 103(50):18951–18956.
28. DeVries I, Ferreiro DU, Sánchez IE, Komives EA (2011) Folding kinetics of the cooperatively folded subdomain of the IκBα ankyrin repeat domain. *J Mol Biol* 408(1):163–176.
29. Trelle MB, et al. (2016) Binding of NFκB appears to twist the ankyrin repeat domain of IκBα. *Biophys J* 110(4):887–895.
30. Dembinski H, et al. (2014) Predicted disorder-to-order transition mutations in IκBα disrupt function. *Phys Chem Chem Phys* 16(14):6480–6485.
31. Cervantes CF, et al. (2009) Functional dynamics of the folded ankyrin repeats of I kappa B alpha revealed by nuclear magnetic resonance. *Biochemistry* 48(33):8023–8031.
32. Studer SM, Joseph S (2007) Binding of mRNA to the bacterial translation initiation complex. *Methods Enzymol* 430:31–44.
33. Mulvihill MM, Guttman M, Komives EA (2011) Protein interactions among Fe65, the low-density lipoprotein receptor-related protein, and the amyloid precursor protein. *Biochemistry* 50(28):6208–6216.
34. Wales TE, Fadgen KE, Gerhardt GC, Engen JR (2008) High-speed and high-resolution UPLC separation at zero degrees Celsius. *Anal Chem* 80(17):6815–6820.